Int. J. Bio-Inorg. Hybd. Nanomat., Vol. 2, No. 1 (2013), 271-280

International Journal of Bio-Inorganic Hybrid Nanomaterials

An Investigation on Synthesis and Magnetic Properties of Manganese Doped Cobalt Ferrite Silica Core-Shell Nanoparticles for Possible Biological Application

Somayyeh Rostamzadehmansour[1*], Mirabdullah Seyedsadjadi[2], Kheyrollah Mehrani[3]

[1] Ph.D., Department of Chemistry, Ardabil Branch, Islamic Azad University, Ardabil, Iran

[2] Associated Professor, Department of Chemistry, Science and Research Branch, Islamic Azad University, Tehran Iran

[3] Assistant Professor, Department of Chemistry, Science and Research Branch, Islamic Azad University, Tehran Iran

Received: 20 November 2012; Accepted: 28 Jannuary 2013

ABSTRACT

In this work, we investigated synthesis, magnetic properties of silica coated metal ferrite, ($CoFe_2O_4$)/SiO_2 and Manganese doped cobalt ferrite nanoparticles ($Mn_xCo_{1-x}Fe_2O_4$ with x= 0.02, 0.04 and 0.06)/SiO_2 for possible biomedical application. All the ferrites nanoparticles were prepared by co-precipitation method using $FeCl_3.6H_2O$, $CoCl_2.6H_2O$ and $MnCl_2.2H_2O$ as precursors, and were silica coated by Stober process in directly ethanol. The composition, phase structure and morphology of the prepared core-shell cobalt ferrites nanostructures were characterized by powder X-ray diffraction (XRD), Fourier Transform Infra-red spectra (FT-IR), Field Emission Scanning Electron Microscopy and energy dispersive X-ray analysis (FESEM-EDAX). The results revealed that all the samples maintain ferrite spinel structure. While, the cell parameters decrease monotonously by increase of Mn content indicating that the Mn ions are substituted into the lattice of $CoFe_2O_4$. The magnetic properties of the prepared samples were investigated at room temperature using Vibrating Sample Magnetometer (VSM). The results revealed strongly dependence of room temperature magnetic properties on (1) doping content, x; (2) particles size and ions distributions.

Keyword: Magnetic properties; Silica coated magnetic nanoparticles; Manganese doped ferrite nanoparticles; Core-Shell.

1. INTRODUCTION

A survey on the scientific literature indicates lots of the researches have been devoted to the synthesis of magnetic NPs, with spinel ferrite structures because of their broad applications in several technological fields including permanent magnets, magnetic fluids, magnetic drug delivery, and high density

(*) Corresponding Author - e-mail: Rostam_Somayyeh@yahoo.com

recording media [1-4]. Structure of these magnetic ferrite NPs, MFe_2O_4 (M= Fe, Co), is cubic inverse spinel formed by oxygen atoms in a closed packing structure where, M^{2+} and Fe^{3+} occupy either tetrahedral or octahedral sites. Interesting point is that, the magnetic configuration in these kinds of materials can be engineered by changing or adjusting the chemical identity of M^{2+} to provide a wide range of magnetic properties [5, 6]. There are many reports about this area in literature. According to one of the recent research studies, substitution of Co^{2+} in $CoFe_2O_4$ nanoparticle structure with Zn^{2+} ($Zn_xCo_{1-x}Fe_2O_4$) exhibited improvement in properties such as excellent chemical stability, high corrosion resistivity, magneto crystalline anisotropy, magneto striation, and magneto optical properties [7-13]. A very interesting point in all of these reports and in many of applications is that, the synthesis of uniform size nanoparticles is of key importance, because the nanoparticles magnetic properties depend strongly on their dimensions. Therefore recently great efforts have been made by various groups to achieve a fine tuning of the size of ferrite and substituted nanoparticles employing different synthesis techniques. In other studies, magnetic properties of cobalt ferrite and silica coated cobalt ferrite were studied [14, 15], but the novelty of this work was that we attempted to study magnetic properties of manganese doped derivatives (Mn_xCo_{1-x} Fe_2O_4 with x= 0.02, 0.04 and 0.06)/ SiO_2 for possible biomedical application. Silica and its derivatives coated onto the surfaces of magnetic nanoparticles may change their particles surface properties and provide a chemically inert layer for the nanoparticles, which is particularly useful in biological systems [16-17].

2. EXPERIMENTAL

2.1. Materials

All chemicals were of analytical grade and were used without further purification. Cobalt chloride hexa hydrate ($CoCl_2.6H_2O$), ferric chloride hexa hydrate ($FeCl_3.6H_2O$), sodium hydroxide (NaOH), Ammonia solution (25%), cetyltrimethylammonium bromide (CTAB) and tetraethyl orthosilicate (TEOS), anhydrous ethanol (C_2H_5OH), were purchased from MERCK company. Deionized water was used throughout the experiments.

2.2. Synthesis of $CoFe_2O_4$

Cobalt ferrite nanoparticles, $CoFe_2O_4$ was synthesized via a coprecipitation method by adding a mixture of 2.5 mL of $CoCl_2.6H_2O$ (0.5 M) and 5 mL of $FeCl_3.6H_2O$ (0.5 M) into a solution mixture of 1 g CTAB in 20 mL distilled water and 5 mL of sodium hydroxide solution (3 M) and stirred under nitrogen protection for 10 min. The resulting black solution was then maintained at 70°C for 1 h and cooled at room temperature. Stable colloidal solution was then separated by centrifugation and the black products obtained were washed by distilled water for several times and dried at room temperature [18].

2.3. Synthesis of $Mn_xCo_{1-x}Fe_2O_4$ nanoparticles

The above described experiments were repeated for preparation of $Mn_xCo_{1-x}Fe_2O_4/SiO_2$ nanoparticles by adding a mixture of 2.5 mL of $CoCl_2.6H_2O$ (1-x) M, 5 mL of $FeCl_3.6H_2O$ (0.5M) and 2.5 mL of $MnCl_2.2H_2O$ (xM) with (x= 0.02, 0.04, 0.06) into a solution mixture of 1 g CTAB in 20 mL distilled water and 5 mL of sodium hydroxide solution (3 M) and stirred under nitrogen protection for 10 min [19].

2.4. Synthesis of Core-Shell $CoFe_2O_4/SiO_2$ and $Mn_xCo_{1-x}Fe_2O_4/SiO_2$ nanoparticles

Silica coated magnetic nanoparticles were prepared using a modified Stober method by dispersing of the prepared nanoparticles in 200 mL of ethanol and adding then 2 mL of 25% ammonia, 20 mL of deionized water and 2 mL of TEOS respectively. The mixture was degassed and stirred vigorously at 50°C for 3 h under nitrogen gas protection to obtain core-shell nanoparticles of $CoFe_2O_4/SiO_2$ and $Mn_xCo_{1-x}Fe_2O_4/SiO_2$. The products obtained were separated and washed with ethanol and water for several times and dried at 40°C for 24 h [20].

2.5. Characterization

X-ray diffraction patterns (PW 1800 PHILIPS), Energy Dispersion Spectrum (Hitachi F4160, Oxford), and FT-IR spectra (A NICOLET 5700) were used to determine the crystal structure of the silica coated Fe_3O_4 nanoparticles and the chemical bonds of Fe-O-Si, respectively. The magnetic properties were analyzed with a Vibration Sample Magnetometer (VSM, Quantum Design PPMS-9).

3. RESULT AND DISCUSSIONS

3.1. XRD characterization

Figure 1 left (a, b, c and d) show X-ray diffraction patterns of $CoFe_2O_4$ and $Mn_xCo_{1-x}Fe_2O_4$ (with x= 0.02, 0.04 and 0.06) nanoparticles. The peaks observed in these patterns assigned to scattering from the planes of (220), (311), (400), (422), (511) and (440), all were consistent with those of standard XRD pattern of spinel, $CoFe_2O_4$ (JCPDS card No. 86-2267) and confirm that all the prepared samples maintain ferrite spinel structure. While, the cell parameters decrease monotonously with the increase of Mn content indicating that Mn ions are substituted into the lattice of $CoFe_2O_4$. The average of crystalline size of $CoFe_2O_4$, $Mn_xCo_{1-x}Fe_2O_4$ nanoparticle at the characteristic peak (311) were calculated by using Scherrer formula. The results of D values, using 311 planes of the spinel structures were 13.36, 35.4 and 30.26 nm respectively. Figure 1 right (a, b) shows X-ray diffraction patterns of $CoFe_2O_4$ and $CoFe_2O_4/SiO_2$ nanoparticles. All the peaks observed in these patterns were consistent with those of standard XRD pattern reported data (JCPDS card No. 86-2267) and confirm crystallinity of $CoFe_2O_4$ and $CoFe_2O_4/SiO_2$ nanoparticles. In addition to the characteristic diffraction peaks of spinel phase, a wide peak appeared at about 2θ= 22-25° (Figure 2b) can be related to the formation of a SiO_2 phase due to the addition of TEOS in basic condition.

3.2. FT-IR spectra

Figure 2 (a, b) represents FT-IR spectra of the $CoFe_2O_4$ and $CoFe_2O_4/SiO_2$ nanoparticles. The strong peaks at about 592 cm^{-1} and 516 cm^{-1} (in Figure 2a) are due to the stretching vibrations of Fe-O and Co-O bonds and the peaks around

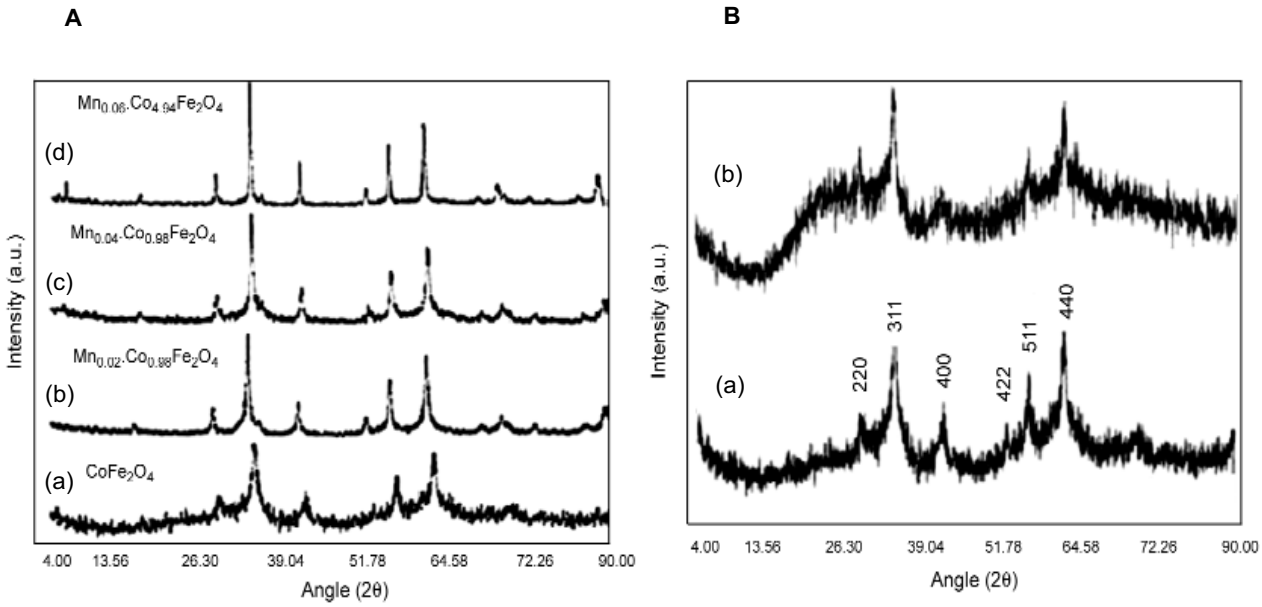

Figure 1 A: *XRD patterns of: a) $CoFe_2O_4$, b, c, d) $Mn_xCo_{1-x}Fe_2O_4$ (with x= 0.02, 0.04 and 0.06);* ***B:*** *a) $CoFe_2O_4$; b) $CoFe_2O_4/SiO_2$. Peak broadening observed in SiO_2 coated nanostructures can be related to the decrease in crystallinity.*

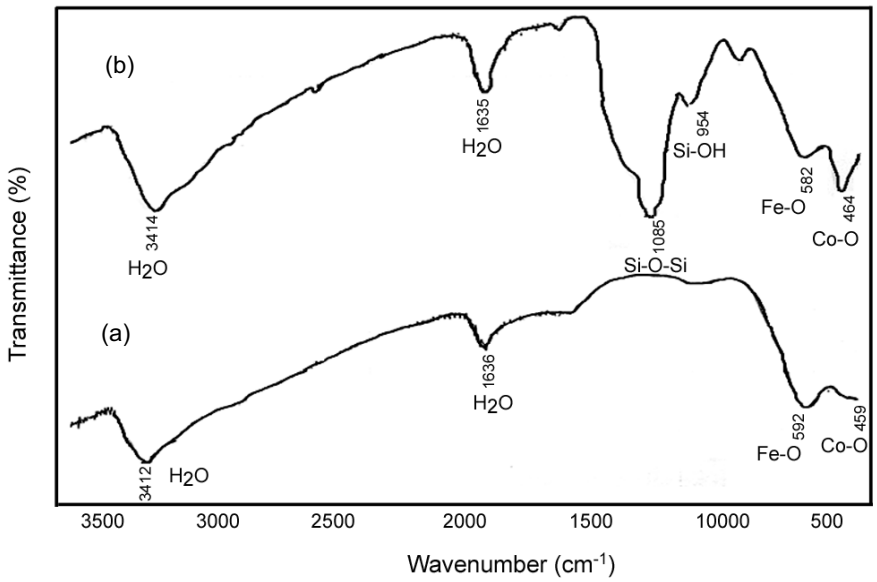

Figure 2: *FT-IR spectrum of (a) $CoFe_2O_4$ and (b) $CoFe_2O_4/SiO_2$ nanoparticles*

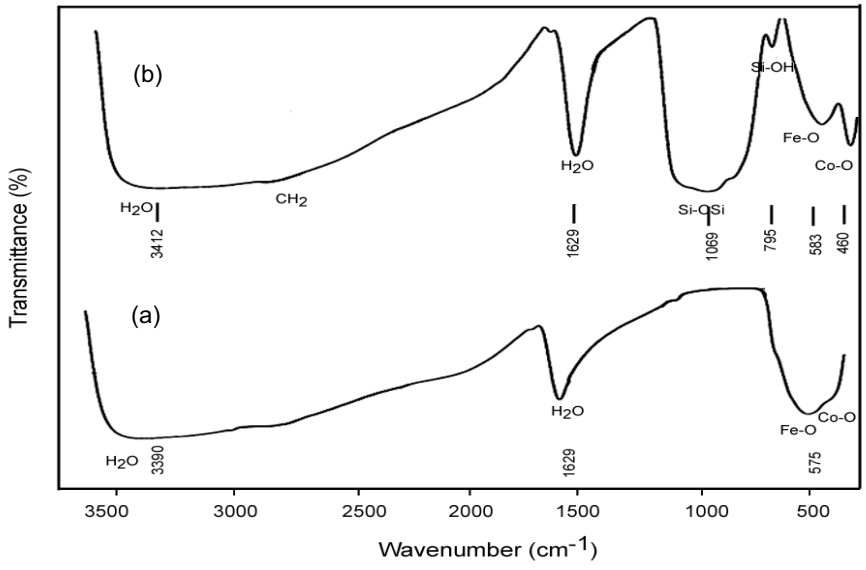

Figure 3: *FT-IR spectrum of (a) $Mn_{0.02}Co_{0.98}Fe_2O_4$ and (b) $Mn_{0.02}Co_{0.98}Fe_2O_4/SiO_2$ nanoparticles*

3000-3500 cm^{-1} and 1624 cm^{-1} have been assigned to the stretching and bending vibrations of the H-O-H bond, respectively, showing the physical absorption of H_2O molecules on the surfaces. In Figure 2b shows IR spectrum of silica coated $CoFe_2O_4$ nanoparticles confirms the presence of the finger print bands below 1100 cm^{-1} which are characteristic of asymmetric (1085 cm^{-1}) and symmetric (810 cm^{-1}) stretching vibrations of framework Si-O-Si.

Figure 3 (a, b) represents FT-IR spectra of the $Mn_{0.02}Co_{0.98}Fe_2O_4$ and $Mn_{0.02}Co_{0.98}Fe_2O_4/SiO_2$

nanoparticles. The strong broad peaks at about 592 cm^{-1} and 516 cm^{-1} (in Figure 3a) are due to the stretching vibrations of Fe-O and Co-O bonds and the peaks around 3000-3500 cm^{-1} and 1624 cm^{-1} have been assigned to the stretching and bending vibrations of the H-O-H bond, respectively, showing the physical absorption of H_2O molecules on the surfaces. In Figure 3b shows IR spectrum of

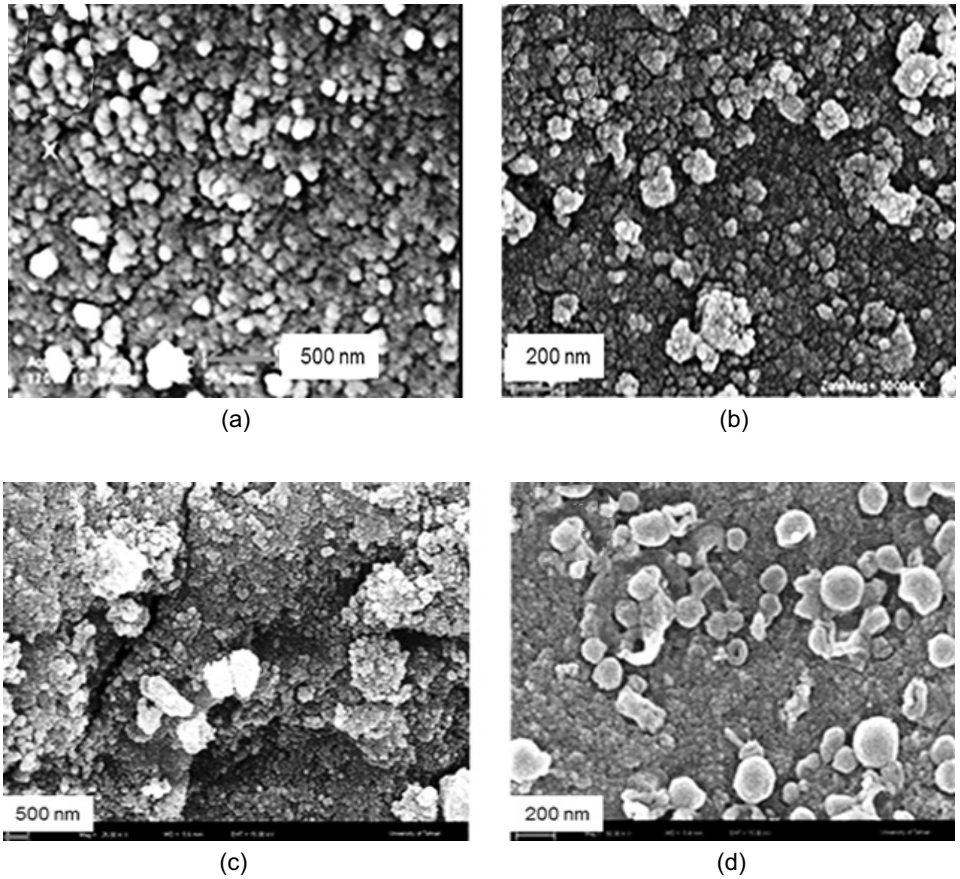

Figure 4: *FESEM images of: a) $CoFe_2O_4$; b) $CoFe_2O_4$ /SiO_2 core-shell nanoparticles; c) $Mn_{0.02}Co_{0.98}Fe_2O_4$; and d) $Mn_{0.02}Co_{0.98}Fe_2O_4$ /SiO_2 core-shell nanostructures.*

Table 1: *EDAX ZAF quantification (standardless) element normalized for $CoFe_2O_4$ and $CoFe_2O_4$ /SiO_2 nanoparticles.*

Sample	Element	wt%	At%
$CoFe_2O_4$	Fe_2O_3 CoO	64.89 35.11	46.45 53.55
$CoFe_2O_4/SiO_2$	Fe_2O_3 CoO SiO_2	46.58 28.61 5.62	30.68 17.86 7.36

Table 2: *EDAX ZAF quantification (standardless) element normalized for $Mn_{0.02}Co_{0.98}Fe_2O_4$ and $Mn_{0.02}Co_{0.98}Fe_2O_4$ nanoparticles.*

Sample	Element	wt%	At%
$Mn_{0.02}Co_{0.98}Fe_2O_4$	Fe	46.83	35.32
	Co	28.49	20.30
	O	13.44	35.28
	Mn	9.12	6.98
Total		100	100
$Mn_{0.02}Co_{0.98}Fe_2O_4/SiO_2$	Fe	48.88	41.84
	Co	28.41	23.o4
	Mn	8.31	7.23
	O	4.07	12.17
	Si	8.42	14.32
Total		100	100

silica coated $Mn_{0.02}Co_{0.98}Fe_2O_4/SiO_2$ nanoparticles confirms the presence of the finger print bands below 1100 cm^{-1} which are characteristic of asymmetric (1085 cm^{-1}) and symmetric (810 cm^{-1}) stretching vibrations of framework Si-O-Si, that confirms the formation of manganese ferrite.

3.3. FESEM and EDAX

Figure 4 (a, b) represents FESEM images of $CoFe_2O_4$ and $CoFe_2O_4/SiO_2$ core-shell nanoparticles. These images show well homogeneous distribution of spheric nanoparticles in the prepared samples. Elemental analysis data (EDAX) for these two composite materials is given in Table 1.

Figure 4 (c, d) represents the FESEM images of $Mn_{0.02}Co_{0.98}Fe_2O_4$ and (b) $Mn_{0.02}Co_{0.98}Fe_2O_4/SiO_2$ nanostructures. These images clearly show also well distributed particles of Mn doped nanostructures in $Mn_{0.02}C_{o0.98}Fe_2O_4$, and in its silica coated nanoparticles, $Mn_{0.02}Co_{0.98}Fe_2O_4$ $/SiO_2$. X-ray dispersive analysis data for these two nanostructure is represented in Table 2. This results confirm presence of Co, Fe, Mn and silica in the related nanoparticles.

3.4. Magnetic properties of $CoFe_2O_4$ nanoparticles

Figure 5 (a, b and c) and Table 3 represent magnetic field dependent magnetization parameters, M(H) for $CoFe_2O_4$ in the size of 13.26, 21.06

Table 3: *Magnetic parameters of $CoFe_2O_4$ in different sizes and $CoFe_2O_4/SiO_2$ nanoparticles.*

$CoFe_2O_4$ nanoparticles	Average particle size XRD (nm)	Saturation magnetization Ms(emu/g)	Remanent magnetization Mr(emu/g)	Coercivity Hc (Oe)	Remanence ratio (Mr/Ms)	Ms emu/g (Bulk)	Mr/Ms (Bulk)
$CoFe_2O_4$	13.26	32.1	0	240	0	80.8	0.84
$CoFe_2O_4$	21.06	12.74	5	2000	0.47	80.8	0.84
$CoFe_2O_4$	34	10.58	4.9	2300	0.46	80.8	0.84
$CoFe_2O_{0.84}/SiO_2$	15.14	8.5	0	50	0	80.8	0.84

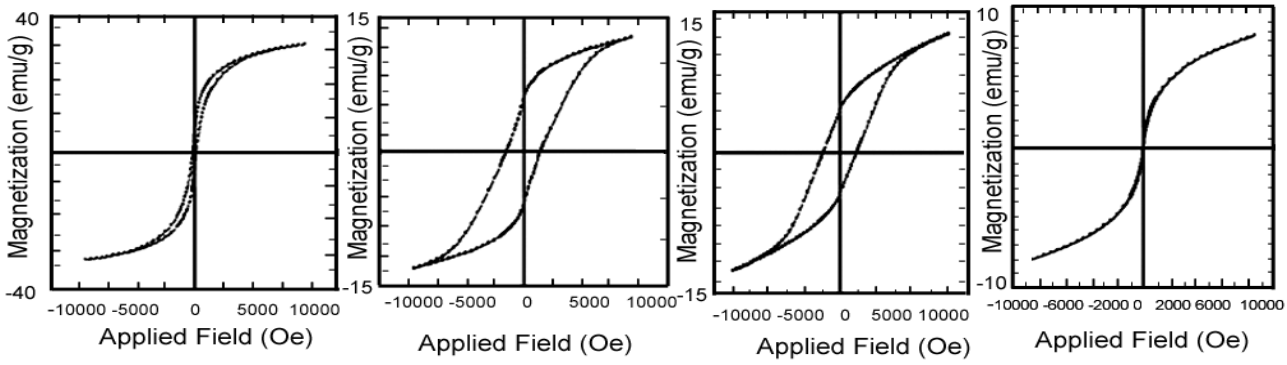

Figure 5: *Magnetization curves versus applied field for synthsized $CoFe_2O_4$ in a size of: a) 13.26 nm; b) 21.06 nm; c) 34 nm; d) 15.4 nm for silica caoted $CoFe_2O_4$ at 300 K in a magnetic field of 15 kOe.*

and 34 nm at room temperature, using vibrating sample magnetometer with a peak field of 15 kOe. The hystersis loops for $CoFe_2O_4$ in the size of 13.26 nm, with a finite low value of coercivity (Hc= 240 Oe) and remanence (Mr= 0) indicate a ferromagnetism at 300 K. Shi-Yong Zhao et al., have reported the same results for their prepared $CoFe_2O_4$ nanoparticles in the size of 14.8 nm and proposed a superparamagnetism properties at the same condition [21]. These results seems contraversal since superparamagnetic particles shohld exhibit no remanence or coercivity, or there are no hysteresis in the magnetization curve. A very important parameter that has to be considered for this kind of materials is coercivity. Coercivity is the key to distinguish between hard and soft phase magnetic materials. Materials with a typically low intrinsic coercivity less than 100 Oe, with a high saturation ted magnetization Ms and low Mr are magnetically called soft and materials that have an intrinsic coercivity of greater than 1000 Oe, typically high remanance, Mr are hard magnetic materials.

So, $CoFe_2O_4$ in the size of 13.26 nm with a low finite value of coercivity and remanance (Mr); (Hc= 240 Oe; Mr= 0.0 emu/g can be considered as a good example for weak ferromagnetism. Whereas, $CoFe_2O_4$ nanoparticles, in the sizes of 21.06 and 34 nm with a high coercivity (Hc= 2000-2500 (Oe) and remanance (Mr) (Hc= 5000 Oe; Mr= 5.0 emu/g, are magnetically hard magnetic materials. A new interesting change on the hystersis loop is observed for silicad coated. $CoFe_2O_4/SiO_2$ (Figure 3d) with a saturation magnetization decreased to 8.5 emu/g and a finite zero value for coercivity (Hc) and remanence (Mr); (Hc= 50 Oe; Mr= 0.0 emu/g) indicating a soft ferromagnetism at RT. Decrease of magnetic saturation in this case can be related to the separation of neighbors nanoparticle by a layer silica leading to the decrease of magnetostatic coupling between the particles.

A closer look at the above mentioned results confirm that magnetic properties of small ferromagnetic particles such as coercivity, as reported by other autors [22, 23], are dominated by two key features: (1) a size limit that below which the specimen cannot be broken into domains, hence it remains with single domain; (2) the thermal energy in the small particles which give rise to the phenomenon of superparamagnetism. These two key features are represented by two key sizes (on length scale): the single domain size and superparamagnetic size (Figure 5) [22, 23].

3.5. Magnetic properties of ($Mn_{0.02}Co_{0.98}Fe_2O_4$) nanoparticles

Figure 6 and Table 4 Compare field dependent magnetization parameters for $CoFe_2O_4$, $Mn_{0.02}Co_{0.98}$ Fe_2O_4 and $Mn_{0.02}Co_{0.98}Fe_2O_4/SiO_2$ nanoparticles in a similar sizes. The hystersis loop for $Mn_{0.02}Co_{0.98}Fe_2O_4$ show a saturation magnetization, Ms of 35.0 emu/g for a size of 35.30 nm and

Table 4: *Magnetic parameters of $Mn_{0.2}Co_{0.98}Fe_2O_4$ and $Mn_{0.2}Co_{0.98}Fe_2O_4/SiO_2$ nanoparticles.*

$CoFe_2O_4$ nanoparticles	Average particle size XRD (nm)	Saturation magnetization Ms(emu/g	Remanent magnetization Mr(emu/g)	Coercivity Hc (Oe)	Remanence ratio (Mr/Ms)
$CoFe_2O_4$	34	10.85	4.9	2500	0.46
$Mn_{0.02}Co_{0.98}Fe_2O_4$	35.30	35	12	500	0.37
$Mn_{0.2}Co_{0.98}Fe_2O_4/SiO_2$	37	3.5	0.75	250	0.21

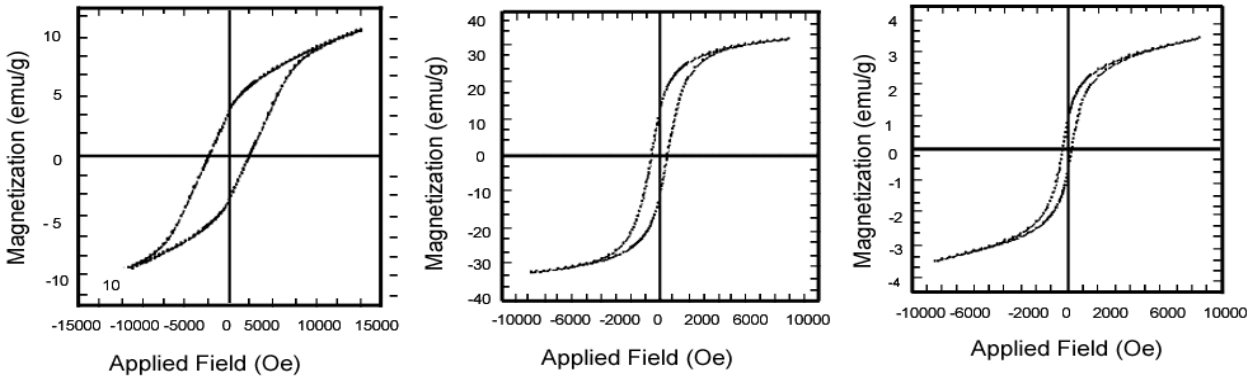

Figure 6: *Magnetization curves versus applied field for synthsized: a) $CoFe_2O_4$; b) $Mn_{0.02}Co_{0.98}Fe_2O_4$ and c)$Mn_{0.02}Co_{0.98}Fe_2O_4/SiO_2$ in the similar size at 300 K in a magnetic field of 15 kOe.*

a finite low value of coercivity (Hc) with increased remanence (Mr); (Hc= 500 Oe; Mr= 12.0 emu/g). The large value of HC for $CoFe_2O_4$ is known to be originated from the anisotropy of the octahedral Co^{2+} ion [24]. So, decrease of HC for Mn doped material can be attributed to a decrease in the octahedral Co^{2+} ions due to their migration to tetrahedral sites. The increase in MS in doped material can also be explained in terms of the Co^{2+} migration [25]. Decrease of the saturation magnetization, remanence (Mr) and coercivity to 250 Oe (Hc= 250 Oe; Mr= 0.75 emu/g), for $Mn_{0.02}Co_{0.98}Fe_2O_4/SiO_2$ due to the surface coating effects has been explained via different mechanisms, such as existence of a magnetically dead layer on the particles surface, the existence of canted spins, or the existence of a spin-glass-like behavior of the surface spins [26]. However, a silica coating can be used to tune the magnetic properties of nanoparticles, since the extent of dipolar coupling is related to the distance between particles and this in turn depends on the thickness of the inert silica shell [27]. A thin silica layer will separate the particles, thereby preventing a cooperative switching which is desirable in magnetic storage data. The MS of the $Mn_xCo_{1-x}Fe_2O_4$ films is seen to increase with increasing x. Also, the coercive field (HC) is found to decrease with increasing Mn doping as shown in Table 6, while the MS increases gradually with x. The large HC of $CoFe_2O_4$ is known to originate from the anisotropy of the octahedral Co^{2+} ion. Thus, the decrease in HC with increasing x is attributed to a decrease in the octahedral Co^{2+} ions due to their migration to tetrahedral sites. The increase in MS can also be explained in terms of the Co^{2+} migration.

4. CONCLUSIONS

- ✓ In this study, the process of preparing hard and soft magnetic nanoparticles having potential for many technological applications such as ultra high density recording media, biotechnology ferrofluids, and fabrication of exchange coupled nanocomposite has been explained.
- ✓ The synthesis processes explored in this study are simple and easy to achieve the desired particle size distribution.
- ✓ Characterization of the prepared cobalt ferrite and Manganese doped cobalt ferrite nano-particles were performed using XRD, FTIR and FESM-EDAX technigues.
- ✓ The magnetic properties of the cobalt ferrite and Manganese doped cobalt ferrite nanoparticles evaluated by VSM and the decreases of satura-tion magnetization with increasing SiO_2 coatings were reported earlier separately by authors [24].
- ✓ Magnetic properties of small ferromagnetic particles such as coercivity, are dominated by two key features: the single domain size and superparamagnetic size.
- ✓ The magnetic measurements on these particles showed strong dependence of the magnetic properties with the particle size.
- ✓ A size limit exist for $CoFe_2O_4$ nanoparticles and cobalt ferrite with size greater than 12 nm showed ferromagnetic behavior at room temperature.
- ✓ High coercivity values higher than 1 kOe and 2-2.5 kOe were obtained for 21.06 and 34 nm $CoFe_2O_4$ nanoparticles at room temperature.
- ✓ Room temperature magnetic properties strongly depend on (1) doping content (x) (2) particles size and ions distributions.
- ✓ The saturation magnetization is strongly dependent on the Mn doping content, x and increased average magnetic moment improved for $Mn_{1-x}Co_xFe_2O_4$ (x= 0.02), have been decreased by Mn content due to the antiferro magnetic super exchange interaction with in the neighbor Mn^{2+} ions through O^{2-} ions for the samples with higher Mn doping.

ACKNOWLEDGMENTS

The authors express their thanks to the vice presidency of Islamic Azad University, Science and Research Branch and Iran Nanotechnology Initiative for their encouragement, and financial supports.

REFERENCES

1. Amstad E., Textor M. and Reimhult E., *Nanoscale*, **3**(2011), 2819.
2. Cheng F.Y., Su C.H., Yang Y.S., Yeh C.S., Tsai C.Y., Wu C.L., Wu M.T., Shieh D.B., *Biomaterials*, **26**(2005), 729.
3. Desantis C., Siegel R., Bandi P., Jemal A., *CA Cancer J. Clin*, (2011), 20134.
4. Chen J., *J. Inorg. Mater*, **24**(5) (2009), 967.
5. Sun Sh., Zeng H., Robinson D.B., Raoux S., Rice P.M., Wang Sh.X., and Li G., *J. Appl. Chem. Soc.*, **126**(2004), 273
6. Giri J., Pradhan P., Somani V., *J. Magn. Magn. Mater*, **320**(5) (2008), 724.
7. Vaidyanathan G., Sendhilnathan S., *Phys B: Phys Condens Matter*, **403**(2008), 2157.
8. Akther Hossain A.K.M., Tabata H., Kawai T., *J. Magn. Magn. Mater*, **320**(6) (2008), 1157.
9. Islam M.U., Aen F., Niazi S.B., Azhar Khan M., Ishaque M., Abbas T., Rana M.U., *Mater Chem Physic*, **109**(2-3) (2008), 482.
10. Arulmurugan R., Vaidyanathan G., Sendhilnathan S., Jeyadevan B., *J. Magn. Magn. Mater*, **303**(1) (2006), 131.
11. Tawfik A., Hamada I.M., Hemeda O.M., *J. Magn. Magn. Mater*, **250**(2002), 77.
12. Kim C.K., Lee J.H., Katoh S., Murakami R., Yoshimura M., *Mater Res Bull*, **36**(12) (2001), 2241.
13. Hou C., Yu H., Zhang Q., Li Y., Wang H., *J. Alloy Compd*, **491**(1-2) (2010), 431.
14. Gharagozlou M., *Chem Cent J.*, 5 (19) (2011), 1.
15. Rostamzademansour S., Sadjadi M.S., Zare K., *Int. J. Nano Dimens,* **4**(1) (2013), 51.
16. Lu Q.H., Yao K.L., Xi D., Liu Z.I., Luo X.P.,

Ning Q., *Nanoscience*, **11**(4) (2006), 241.
17. Deng Y.H., Wang C.C., Hu J.H., Yang W.L., Fu S.K., *Colloids Surfaces A: Physicochem. Eng Aspects*, **262**(2005), 87.
18. Parekh K., *Indian J. Pure & Appl Phys*, **48**(4) (2010), 581.
19. Girgis E., Wahsh M.M., Othman A.G., Bandhu L., Rao K., *Nanoscal Res Lett.*, **6**(1) (2011), 460.
20. Li Y.S., Church J.S., Woodhead A.L., Moussa F., *Spectrochimica Acta Part A*, **79**(1) (2010), 484.
21. Sounderya N., Zhang Y., *Rec. Paten. Biomed. Eng*., **1**(1) (2008), 34.
22. Zhao S.Y., Lee D. K., Kim C.W., Cha H.G., Kim Y.H., and Kang Y.S., *Bull. Korean Chem. Soc*., **27**(2006), 237.
23. B.D. Cullity, 1972. *Introduction to Magnetic Materials,* Addison-Wesley Publishing.
24. J. Kenneth, 2001. *Nanoscale Materials in Chemistry,* John & Sons, Inc.
25. Zhou B., Zhang Y.W., Yu Y.J., Liao C.S., Yan C.H., Chen L.Y., and Wang S.Y., *Phys. Rev. B*, **68**(2003), 024426.
26. Joo K.K., Kim H.K., Park Y.R., *J. Kore. Phys. Soc*., **49**(2006), 1024.
27. Kodama R.H., *J. Magn. Magn. Mater*, **200**(1999), 359.